Metabolomic profiling reveals effects of marein on energy metabolism in HepG2 cells

Baoping Jiang [1)], Liang Le [2),3) #], Keping Hu [1)], Lijia Xu [1)], Peigen Xiao [1)#]

[1)] Institute of Medicinal Plant Development (IMPLAD), Chinese Academy of Medical Sciences and Peking Union Medical College, Beijing 100193, China;

[2)]Institute of Chinese Materia Medica，China Academy of Chinese Medical Sciences，Beijing 100700，China;

[3)]Post-doctoral Scientific Research Center，China Academy of Chinese Medical Sciences，Beijing 100700，China;

Corresponding author:

Peigen XiaoP pgxiao@implad.ac.cn, 151 Malianwa North, Haidian District, Beijing 100193, China;

Liang Le llfxcy@163.com, 151 Malianwa North, Haidian District, Beijing 100193, China

Running Head: Metabolomic profiling reveals effects of marein

Abstract:

Previous studies have suggested that *Coreopsis tinctoria* improves insulin resistance in rats fed with high-fat diet. But little is known about the antidiabetic effects of marein which is the main component of *C. tinctoria*. This study investigated the effects of ethyl acetate extract of *C. tinctoria* (AC) on insulin resistance (IR) in rats fed a high-fat diet. High glucose and fat conditions cause a significant increase in blood glucose, insulin, serum TC,TG and LDL-C, leading to an abnormal IR in rats. However, treatment with AC protects against HFD-induced IR by improving fasting serum glucose and lipid homeostasis. High glucose conditions cause a significant decrease in glycogen synthesis and increases PEPCK and G6Pase protein levels and Krebs-cycle-related enzymes levels, leading to an abnormal metabolic state in HepG2 Cells. However, treatment with Marein improves IR by increasing glucose uptake and glycogen synthesis and by downregulating PEPCK and G6Pase protein levels. The statistical analysis of HPLC/MS data demonstrates that Marein restores the normal metabolic state. The results show that AC ameliorates IR in rats and Marein has the potential effect in improving IR by ameliorating glucose metabolic disorders.

Keywords: Metabolomics; Marein; insulin resistance; metabolites; Krebs cycle

Abbreviations: AC, ethyl acetate extract of *Coreopsis tinctoria;* TCA, Tricarboxylic acid; HepG2, hepatocellular carcinoma cell line; 2-NBDG, 2-(N-(7-nitrobenz-2-oxa-1, 3-diazol-4-yl) amino)-2-deoxyglucose; G6Pase, glucose-

6-phosphatase; PEPCK, phosphoenolpyruvate carboxykinase; IR, insulin resistance; HFD, high-fat diet; SDHA, succinate dehydrogenase flavoprotein subunit; ACO2, aconitase 2; IDH2, isocitrate dehydrogenase 2; CS, citrate synthase; FH, fumarate hydratase; MDH2, malate dehydrogenase; DLST, dihydrolipoamide S-succinyltransferase.

Introduction

Type 2 diabetes (T2DM) is a progressive disease characterized by deterioration of glycaemia and escalating therapeutic complexity [1]. In diabetes mellitus, chronic hyperglycemia develops as a consequence of decreased insulin action from impaired insulin secretion and insulin resistance (IR) [2, 3]. Once chronic hyperglycemia is established, it in turn aggravates IR, forming a vicious cycle that is collectively called glucose toxicity[4, 5]. The liver is the primary organ responsible for regulating glucose homeostasis [6]. Hepatic IR leads to altered glucose metabolism and hyperglycemia, which is characterized by the inability of insulin to inhibit hepatic gluconeogenesis by suppressing unidirectional enzymes, namely, phosphoenolpyruvate carboxykinase (PEPCK) and glucose 6-phosphatase (G-6Pase)[7, 8]. G-6Pase plays a role in glucose homeostasis [9]. PEPCK is a key rate-limiting enzyme of gluconeogenesis. The activities of G-6Pase and PEPCK are increased significantly in the liver of diabetic rats [8]. Inhibition of G-6Pase and PEPCK enzymes may interfere with gluconeogenesis and can be useful in treating diabetic hyperglycemia [10-13]. In the liver mitochondrial PEPCK (PEPCK-M)adjoins its profusely studied cytosolic isoform (PEPCK-C) potentiating gluconeogenesis and TCA flux, so hepatic PEPCK is required to sustain the

Krebs cycle [14]. In addition, the Krebs cycle completes the oxidation of glucose and plays an important role in the glucose metabolism. Therefore, methods that enable simultaneous measurement of numerous cellular metabolic intermediates in gluconeogenesis and the Krebs cycle are required to elucidate the mechanisms of glucose metabolism disorders.

Metabolomics is a top-down systems biology approach whereby metabolic responses to biological interventions or environmental factors are analyzed and modeled [15]. Metabolomics measures perturbations in metabolites reflecting changes of metabolism caused by environmental factors, and provides insights into the global metabolic status of the entire organism by monitoring the entire pattern of low molecular weight compounds rather than focusing on an individual metabolic intermediate [16]. Deregulations of metabolic processes are expected to be directly or related with relevant disease end-points, which are represented by the levels of metabolites [17]. Recent longitudinal metabolomic studies have found correlations between circulating metabolites and prediabetes, future development of IR, or type 2 diabetes in humans. For example, increasing in circulating aromatic amino acids (AAAs) and branched-chainamino acids (BCAAs) are biomarkers of risk [9, 18, 19].

Coreopsis tinctoria Nutt. (Asteraceae), a traditionally used preparation for diabetes treatment in Portugal [20, 21], is a plant native to North America that has spread worldwide. Our previous study showed that *C. tinctoria* increases insulin sensitivity and regulates hepatic metabolism in rats fed a high-fat diet [22].Since these activities are closely related to metabolic regulation and IR, we tried to identify the protective effect of ethyl acetate extract of *C. tinctoria* Nutt

(AC) on IR, and its possible mechanism of action. Chalcones (okanin and butein derivatives) are the main constituents of ethyl acetate extract of *C. tinctoria* and among them, identified Marein (okanin-4'-O-*β*-D-glucopyranoside) as the main metabolite [23]. Marein has many beneficial biological activities, including antihyperlipidemic [24], antioxidative [25], antidiabetic [26], and antihypertensive effects [27]. Previous research has also found that Marein prevented tert-Butyl-Hydroperoxide and cytokine induction in a mouse insulinoma cell line (MIN6) through the inhibition of the apoptotic signaling cascade[20]. In addition, Marein promotes pancreatic function recovery in streptozotocin-induced glucose-intolerant rats [26, 28]. Our previous studies found that Marein could be the main active compounds of *C. tinctoria* in improving IR[29]. The protective effects of marein on high glucose-induced metabolic disorder via IRS1/AKT/AS160 signal pathway in HepG2 cells[30]. These findings focused on *in vivo* anti-diabetic effect led us to further investigate the underlying mechanism, as to our knowledge no studies on the mechanisms of metabolic disorder of Marein have been reported, especially on energy metabolic level.

In this study, we employed LC/MS-based metabolomics techniques to explore the potential targets and mechanisms of Marein for the attenuating IR and type 2 diabetes. Our study revealed involvement of glucose metabolism and the Krebs cycle in the protective effects of Marein in a high-glucose and fat-induced IR model.

Materials and methods

Materials

The human liver hepatocellular carcinoma cell line HepG2 was purchased from the Cell Bank of the Chinese Academy of Sciences (Beijing). Dulbecco's modified Eagle's medium (DMEM), fetalbovine serum (FBS), and other tissue culture reagents were purchased from Gibco (Life Technologies, USA). Other reagents were purchased from Sigma-Aldrich Co. (St. Louis, MO, USA) unless otherwise indicated. AC was analyzed by HPLC (Waters 2690) with a diode-array detector (Waters 2487) scanning from 200–600 nm. Ethyl acetate extract was seperated by Shim-pack VP-ODS column (150□×□4.6 mm, 5 μm) with the optimum condition as described previously[28, 31]. Marein was extracted from *C. tinctoria Nutt.* by our lab. And we also purchased the compound Marein from Chromadex (00013126-604, California, USA), and the purities exceeded 99%. Deionized water was used in all experiments. All of the other chemicals and reagents were of analytical grade. The following antibodies were used in immunoblotting experiments and at the indicated dilutions: rabbit polyclonal anti-PCK1 (PEPCK) (ab28455, 1:1000), rabbit polyclonal anti-G6Pase (ab83690, 1:1000), rabbit monoclonal anti- aconitase 2 (ACO2) (ab129069, 1:10000), rabbit monoclonal anti- malate dehydrogenase (MDH2) (ab181857, 1:10000), mouse monoclonal anti-isocitrate dehydrogenase 2 (IDH2) (ab184196, 1:1000), mouse monoclonal anti- fumarate hydratase (FH) (ab113963, 1:50000), rabbit polyclonal anti-citrate synthase (CS) (ab96600, 1:1000), mouse monoclonal anti- succinate dehydrogenase flavoprotein subunit (SDHA) (ab14715, 1:10000), rabbit monoclonal anti-SDHB (ab178423, 1:5000, abcam, UK), and anti-β-actin antibody (1:1000, CW0096A, CWBio). Dihydrolipoamide S-succinyltransferase (DLST)

149 ***Animals and drug treatments.***

150 Sprague Dawley rats were randomly divided into six groups of 10 animals
151 each. The control group that was given deionized distilled water to drink and
152 fed standard rat chow 32 composed of 60% vegetable starch, 12% fat, and
153 28% protein. The high-fat diet (HFD) model group[32] that was given deionized
154 distilled water and fed a high fat diet of 60% fat, 14% protein and 26%
155 carbohydrate. The metformin group was administrated with 200 mg/kg of
156 metformin as a positive control by oral gavage and fed a HFD. The rats in the
157 AC three groups were as follows: low dose of AC (150 mg/kg of body weight +
158 HFD), middle dose of AC (300 mg/kg of body weight + HFD), high dose of AC
159 (600 mg/kg of body weight + HFD). The study was approved by the Ethics
160 Committee of the Institute of Medicinal Plant Development, CAMS&PUMC
161 (Beijing, China). All experimental procedures were performed in accordance
162 with relevant guidelines approved by the Ethics Committee of the Institute of
163 Medicinal Plant Development, CAMS&PUMC.

164

165 ***Cell culture and drug treatment***

166 HepG2 cells were cultured in low glucose DMEM (5.5 mmol/L glucose) that
167 was supplemented with 10% FBS and 1% antibiotics at 37°C in humidified air
168 containing 5% CO_2. Cells in the exponential phase of growth were used in all
169 of the experiments. HepG2 cells were grown for 3 days and then divided into
170 different groups for the treatments. The treatment groups (Marein, dissolved
171 in DMSO, not more than 0.5 percent) were as follows: (1) Control: incubated
172 in low glucose DMEM for 72 h; (2) High glucose treatment: incubated in
173 DMEM containing 55 mmol/L glucose for 72 h; (3-6) Marein and glucose

174 treatment: incubated in DMEM containing Marein (40, 20, 10, or 5 μ mol/L) or
175 0.5 mmol/L metformin (Positive control) for 24 h and then incubated in
176 DMEM containing 55 mmol/L glucose for 72 h. 100 nmol/L insulin was added
177 into the all treated group for 30 min before all experiments.

178 ***Detection of glucose uptake***

179 Glucose uptake rate was measured by adding 2-(N-(7-nitrobenz-2-oxa-1,
180 3-diazol-4-yl) amino)-2-deoxyglucose, a fluorescently labeled deoxyglucose
181 analog (2-NBDG, Cayman Chemical), as a tracer to the culture medium as
182 previously reported [33]. 2-NBDG uptake was then measured after stimulating
183 the cells for 15 min with 1×10^{-7} mol/L insulin as our previous described[31]. The
184 cells treated by drugs were then washed twice and incubated with 100 μmol/L
185 of 2-NBDG in glucose-free culture medium for 20 min. The cells cultured in
186 medium without 2-NBDG were used as a negative control. The cells were
187 washed twice prior to fluorescence detection using a microplate reader
188 (Infinite 1000 M, Tecan, AUSTRIA) with fluorescence excitation at 488 nm
189 and emission detected at 520 nm.

190 ***Determination of ATP, pyruvate and lactate concentrations***

191 The cellular ATP content was detected by using an ATP content kit
192 (S0026, Beyotime Institute of Biotechnology, China). Briefly, the cell pellets
193 were collected by centrifugation at 1000 ×*g* for 5 minutes after digestion with
194 0.25% trypsin. The homogenate was incubated in boiling water for 30
195 minutes, and the supernatant was aspirated after centrifugation at 5000 ×*g* for
196 10 minutes. An ATP assay kit was used for all of the samples. The results
197 were analyzed with a luminometer (Fluoroskan Ascent FL, USA).

198 The cellular lactate and pyruvate concentration was detected by using a

lactate assay (A019-2, Nan Jing Jian Cheng Bioengineering Institute, Nan Jing City, China) and pyruvate assay kit (A081, Nan Jing Jian Cheng Bioengineering Institute, Nan Jing City, China) respectively. Briefly, cell pellets were collected by centrifugation at 500 ×*g* for 10 minutes after scraping the cells with a cell scraper. Cells were washed twice with PBS, then resuspended in PBS and lysed with a sonicator. The homogenate was detected using a UV/Visible Spectrophotometer (Lambda 35, Perkin Elmer, USA).

RNA extraction and quantitative real-time PCR (qPCR)

Cells treated with high glucose or Marein were then collected to isolate total RNA. Total RNA was reverse transcribed, and *PEPCK, G6Pase, FH, MDH2, SDHA, SDHB, IDH2, ACO2, CS* and *GAPDH* gene expression was measured by QPCR using iCycler thermocycler (BioRad, Hercules, CA) as previously described [34]. The primers of these genes are listed in the Table 1. All samples were analyzed in triplicate, and the gene expression levels were normalized to control human *GAPDH* values. The relative expression of treated samples was normalized to that of untreated cells according to ΔCt analysis.

Western blot analysis

All immunoblots were of the cell lysate with 1×10^7 cells per sample with RIPA cell lysis buffer (50 mM Tris-HCl, pH 7.4, 1% NP-40, 0.5% Na-deoxycholate, 0.1% SDS, 150 mM NaCl, 2 mM EDTA and 50 mM NaF). PEPCK and G6Pase were detected with anti-PEPCK and anti-G6Pase antibodies respectively, both used at a dilution of 1:1000. FH, MDH2, SDHA, SDHB, ACO2, CS, IDH2 and GAPDH were detected by anti-FH, anti-MDH2,

anti-SDHA, anti-SDHB, anti-ACO2, anti-CS, anti-IDH2 and anti-GAPDH for 4h following the instructions respectively. The secondary antibodies goat anti-mouse IgG and goat anti-rabbit IgG were peroxidase-conjugated at a dilution of 1:10000 and 1:20000 respectively. Immune complexes were visualized with ECL chemiluminescence (GE Healthcare, Little Chalfont, UK). Densitometric analyses were performed with ImageJ2 software for Microsoft Windows.

Metabolite profiling

Metabolite profiling was performed as previously reported [35]. Targeted metabolomic experiment was analyzed by TSQ Quantiva (Thermo, CA). C18 based reverse phase chromatography was utilized with 10mM tributylamine, 15mM acetic acid in water (pH ~6)and 100% methanol as mobile phase A and B respectively. This analysis focused on tricarboxylic acid cycle, glycolysis pathway, pentose phosphate pathway, amino acids and purine metabolism. In this experiment, we used a 25-minute gradient from 5% to 90% mobile B. Positive-negative ion switching mode was performed for data acquisition. Cycle time was set as 1 second and a total of 138 ion pairs were included. The information of partial ion pairs are listed in Table 2. The resolution for quartile 1 and quartile 3 are both 0.7FWHM. The source voltage was 3500v for positive and 2500v for negative ion mode. Sweep gas was turned on at 1(arb) flow rate. In the experiments, metabolites were extracted from 1×10^7 HepG2 cells and finally redissolved in 80 μl of 80% methanol. One microliter of sample was loaded for targeted metabolomics analysis. We used specific sample as quality control (QC) instead of internal standard. Total ion current and chromatographic patterns were evaluated. And Table 3 shows three representative compounds in QC runs.

Statistical analysis

The MS raw data of cellular extracts was processed using Thermo Xcalibur (Thermo, USA). Analyzed spectral data was transformed to contain aligned peak area with the same mass/retention time pair as well as normalized peak intensities and sample name. The main parameters for data processing were set as follows: mass range (80-1200 Da), mass tolerance (5 ppm), intensity threshold (100 counts), retention time (0-20 min) and retention time tolerance (0.2 min). The resulting data were mean-centered and pareto-scaled prior to statistical analysis by Principal Component Analysis (PCA) to differentiate each group. PCA was used to visualize the maximal difference of global metabolic profiles[36]. All data were expressed as means±standard error of the mean (SEM). Statistical significance was calculated with one-way ANOVAs and post hoc Turkey's tests in GraphPad Prism 5.0 (GraphPad Software, San Diego, CA, USA).. Differences were considered to be statistically significant when $P<0.05$. All experiments were performed at least four times.

Results

AC partially improves serum glucose and lipid homeostasis and protects against HFD-induced IR in HFD-fed rats

To explore the effect of AC in rats, we constructed the animal IR model induced by high glucose and fat diet. *The results showed that* the serum total cholesterol (TC) and triglyceride (TG) concentrations were lower than those in the chow diet-fed animals at the end of the 8-week HFD (Fig. 1A and 1B). The analysis of serum lipoproteins revealed that the hypercholesterolemia in rats

fed a HFD was associated with increased low-density lipoprotein-cholesterol (LDL-C) and decreased high-density lipoprotein-cholesterol (HDL-C), typical phenotypes of diabetic dyslipidemia (Fig. 1C and 1D). Treatment with AC for 8 weeks significantly improved the lipid profiles and reduced the serum levels of glucose and insulin. AC or metformin (MET; 200 mg/kg) significantly reduced the fasting glucose and insulin levels (Fig. 1E and 1F). Moreover, treatment with Marein increased insulin sensitivity index and improved the insulin tolerance (Fig. 1G and 1H). Although, HFD rats showed a clear increase in body weight, there are no significantly changes in drug treated group except the positive control compared with HFD group. Histological examination of the liver in HFD-treated rats showed lipid accumulation and fatty degeneration in the hepatocytes; however, treatment with 100 mg/kg marein significantly attenuated the formation of fat vacuoles in the liver sections (Fig. 2).

Marein increases glucose uptake, hexokinase activity, and glycogen synthesis and decreases RNA and protein expression of PEPCK and G6Pase in high-glucose-induced IR model cells

We evaluate the effect of marein (Fig. s1) extracted from *C. tinctoria* on glucose consumption. 55 mmol/L glucose-induced cell model of IR was successfully constructed with HepG2 cells. Glucose decreased 2-NBDG uptake in a both time-dependent and dose-dependent manner (Fig. 3A). The results showed that Marein had a potential effect on promoting the uptake of glucose into HepG2 cells. The dose-dependent effects of Marein treatment for 24h were investigated from 1.25 μmol/L to 40 μmol/L. After treatment with 5 μmol/L of Marein, the 2-NBDG uptake into HepG2 cells reached the highest level, which was the plateau level (Fig. 3B). Then, the effect of Marein on IR

299 induced by high glucose was investigated with 2-NBDG. Pre-treatment of
300 HepG2 cells for 24h with all concentrations of Marein obviously increased
301 glucose uptake that approach to 90.4% of control with 10 μmol/Lol/L Marein
302 (Fig. 3C), although no significant difference of cell survivals were observed in
303 HepG2 cells treatment with Marein (Fig. 3D),. We thus selected 10 and 5
304 μmol/L Marein to use in the subsequent experiments. The IR model with
305 HepG2 cells (55 mmol/L glucose) causes a decrease in the glycogen content
306 and hexokinase (a key enzyme in glycogen synthesis) activity. Both
307 concentrations (5 and 10μmol/L Marein) inhibited the effect of 55 mmol/L
308 glucose (Fig. 3E and 3F). Marein can thus increase hexokinase activity and
309 glycogen synthesis in a dose-dependent manner in an IR model where these
310 were previously suppressed.

311 In the hepatocyte, PEPCK and G6Pase levels and gluconeogenesis are
312 stimulated by inhibition of AKT and are restrained by the synthesis of
313 glycogen in a situation of IR [37]. In this study, 55 mmol/L glucose caused an
314 increase in protein and mRNA levels of PEPCK and G6Pase, but Marein
315 inhibited these alterations (Fig. 3G-I).

316

317 ***Multivariate statistical analysis of HPLC/MS data summarizes metabolic***
318 ***differences in treatment groups***

319 Measured levels of small molecule metabolites of enzymes involved in
320 glucose metabolism and the Krebs cycle are used to verify the changes of
321 these enzymes. Representative HPLC/MS data of cell samples from the high
322 glucose treated cells, control cells and Marein-treated group were used in
323 statistical analysis, as shown in Fig. 4. The three-dimensional PCA score plot

for the first three principal components (PC1, PC2 and PC3) with clustering of each group. The clear separation of the high glucose group and control group suggests that severe metabolic disturbance occurs in the IR model cells (Fig. 4A, 4B). Marein (5 μmol/L and 10 μmol/L) group was clearly separated from the model group (high glucose) and partially overlapped with control group, suggesting Marein had apparent effect on the IR. The PCA score plots of PC1, PC2 and PC3 revealed that data points, each representing one sample, were clustered in a way that allowed Model group (high glucose) to be clearly separated from control, Marein (10 μmol/L), Marein (5 μmol/L) and positive control groups along PC1 (Fig. 4C, 4D, 4E). Changes in important positions in a network more strongly impact the pathway than changes occurring in marginal or relatively isolated positions. MetaboAnalyst 3.0 revealed that differential metabolite content is important for the normal response to high glucose group, and multiple pathways are altered in high glucose and Marein group (Fig. 4F). The impact-value threshold calculated via pathway topology analysis was set to 0.10 [38], and 27 of the regulated pathways were identified as potential target pathways (Fig. 4F and Table 4) of marein in high glucose-induced model.

Furthermore, unsupervised hierarchal cluster analysis revealed the fluctuation of levels across different groups, as visualized by a heat map (Fig. 5A). Metabolic substrates of different treatment groups were changed in different degrees. Z-score plots were constructed to identify metabolic changes distinct between high glucose group and control group. 137 metabolites exclusive to cells after treatment with high glucose (red plot) were identified. However, treatment with 10 μmol/L Marein significantly reduced the

levels of these metabolites (green plot, Fig. 5B).

Effects of Marein on energy metabolism intermediates in high glucose-induced IR model cells.

High glucose-treated cells exhibited changes in the levels of metabolic intermediates that participate in energy metabolism, including the glycolytic pathway and the Krebs cycle. Concentrations of major intermediates involved in glycolysis, such as dihydroxyacetone phosphate (DHAP; 0.48-fold, $p= 8\times10^{-3}$), and 3-phosphoglycerate (0.61-fold, p= 0.04), were significantly decreased in the high glucose group, compared with control group. However, 10 μmol/L Marein reduced the effect of high glucose on these two metabolites (Fig. 6).

The high glucose condition clearly increased levels of other measured Krebs cycle intermediates compared with control group, including citrate (5.09-fold, $p= 1.5\times10^{-7}$), succinate (6.46-fold, $p= 1.7\times10^{-4}$), aconitate (3.11-fold, $p= 5.2\times10^{-6}$), and malate (4.08-fold, $p= 8.8\times10^{-6}$). 10 μmol/L and 5 μmol/L Marein partially decreased the effect of high glucose on these Krebs cycle intermediates.

Marein reduces mRNA and protein expression of Krebs related enzymes SDHA, ACO2, IDH2 and CS in high-glucose-induced IR model cells.

To evaluate the effect of Marein on Krebs cycle metabolism of human hepatocyte exposed to high glucose, the RNA and protein expression of Krebs related enzymes were detected with qPCR and western blot assays. As shown in figure 7A, treatment with 55 mmol/L glucose caused to an increase of some Krebs cycle mRNA levels, including *SDHA*, *ACO2*, *IDH2* and *CS*,

whereas this effect was inhibited by Marein. There were no detectable differences in mRNA levels of *FH*, *MDH2* and *DLST*in the high-glucose-induced IR model cells. In accordance with the results of mRNA expression, the protein levels of SDHA, ACO2, IDH2 and CS were also increased in the treatment group with 55 mmol/L glucose, but FH, MDH2 and SDHB were not altered. Marein reduced the effect of high glucose on the protein expression of SDHA, ACO2, IDH2 and CS in a dose-dependent manner (Fig. 7Band 7C).

Marein reduces ATP levels, pyruvate and lactate concentration in high glucose-induced IR model cells.

As exposure to high glucose will decrease glycogen synthesis, the effect of high glucose on gluconeogenesis was evaluated by detecting the pyruvate and lactate concentration and ATP levels. Under the IR condition, cells produced more ATP to supply energy due to a decline in glucose uptake. Treatment with high glucose also caused the elevation of pyruvate and lactate concentration, whereas this was inhibited by 10 and 5 μmol/L Marein (Fig.7D-F). This result indicates that increased gluconeogenesis plays a key role in the damage caused by high glucose in HepG2 cells, and that Marein can ameliorate that effect.

Discussion

Previous study showed that the flower tea *C. tinctoria* increases insulin sensitivity and regulates hepatic metabolism in rats fed a high-fat diet[22]. In this study, it had been showed that AC strongly improves glucose and lipid homeostasis disrupted by HFD in rats. As the main components of AC, Marein protects HepG2 cells from high glucose-induced glucose metabolism disorder. Metabolomics analyses showed that Marein improves the multitude metabolic

399 pathway including TCA cycle, gluconeogenesis and amino acid metabolism in
400 HepG2 cells. Our results demonstrate that pretreatment of HepG2 cells with
401 Marein significantly reversed high glucose-induced the changes of the key
402 substrates and enzymes in gluconeogenesis and Krebs cycle.

403 The liver plays an important role in maintaining blood glucose
404 concentration both by supplying glucose to the circulation via glycogenolysis
405 and gluconeogenesis and by removing glucose from the circulation to
406 increase glycogen synthesis [37]. We found that glucose utilization and
407 glycogen synthesis were significantly decreased but the activity of PEPCK
408 and G6Pase, the key enzymes in the metabolic pathway of gluconeogenesis
409 were obviously increased in cells treated with high glucose (Fig. 3). These
410 results are in agreement with the previous findings that hepatic IR can be
411 attributed mostly to decreased stimulation of glycogen synthesis by insulin
412 while gluconeogenesis is abnormally enhanced due to the inefficient utility of
413 glucose [39]. Our data showing that pretreatment with Marein significantly
414 reversed the high-glucose-induced decrease in glucose utilization and
415 glycogen synthesis, increasing in the activity of PEPCK and G6Pase.
416 Consistent with the protein expression of gluconeogenesis enzymes, the
417 metabolites of glycolytic and gluconeogenesis pathway were significantly
418 decreased in the high glucose group (Fig.. 3G), which could be reversed by
419 pretreatment with Marein. In accordance with previous reports, pyruvate and
420 lactate were clearly increased in the high glucose treatment cells [40, 41]. These
421 metabolites were the end product of glycolysis, thus their levels elevated in
422 response to an increased glycolytic activity. This is different from the liver
423 tissues with type 2 diabetes [42]. One possible explanation for these results is

that HepG2 cell is a kind of tumor cell line with a high rate of aerobic glycolysis, known as the Warburg effect, which is a hallmark of cancer cell glucose metabolism [43]. Our results demonstrated that pretreatment with Marein before high glucose treatment significantly reduced the high glucose-induced increase in pyruvate and lactate generation and decrease in glycolytic activity in HepG2 cells. It is widely accepted that pyruvate is converted to acetyl-CoA and then enter the Krebs cycle in the mitochondria. Previous reports have demonstrated that the key enzyme activities of the Krebs cycle are significantly altered in type 2 diabetes [35, 44, 45].

In this study, mRNA expression and protein levels of these enzymes were measured, and it was found that treatment with high glucose caused an increase in mRNA and protein levels of some key enzymes including ACO2, IDH2, CS and SDHA, and affected upstream reactions of the Krebs cycle, findings which are in agreement with the previous findings that are mostly focused on the key enzymes activities of Krebs cycle [35, 44, 45]. The high-glucose condition did not affect the enzymes downstream of the Krebs cycle, such as FH and MDH2. *SDHB* gene expression was not affected by high glucose, which may be because SDHB is not the catalyzing subunit (Fig. 7). However over-activation of these enzymes as induced by high glucose may be suppressed by pretreatment with Marein.

A recent report by Choi et al. [46] implicates glucolipotoxicity as a cause for impaired glucose metabolism, leading to a decrease in Krebs cycle intermediates that is consistent with our current findings that the levels of Krebs cycle intermediates, such as succinate, citrate, aconitate, and malate are significantly increased in the high glucose group. On the other hand,

449 pretreatment with Marein before high glucose significantly increased the
450 above Krebs cycle intermediates, which suggested that Marein could
451 significantly increase the rate of the Krebs cycle and the accumulation of
452 these intermediates, and thus reduce the toxicity of glucose. However, our
453 study also found that mRNA and protein levels of Krebs cycle-related
454 enzymes, such as SDHA, CS, ACO2 and IDH2, significantly increased in high
455 glucose group and decreased in Marein pretreatment group, which may
456 reverse the stress response to these substrates. The increase in these
457 enzymes may degrade the related substrates.

458 In summary, we evaluated the effect of marein extracted from on IR. And
459 then we have demonstrated that Marein attenuated the IR induced by high
460 glucose in vitro. Our results show that Marein's improvement of the IR effect
461 can be attributed to it ameliorating numerous high glucose-induced processes
462 such as decrease in glucose uptake and glycogen synthesis, inhibition the
463 activity of hexokinase, perturbation of the glyconeogenesis and Krebs cycle
464 homeostasis, and an increase in the levels of ATP, pyruvate and lactate.
465 Meanwhile, Marein also improves glucose and lipid metabolism disorder
466 disrupted by HFD in rat IR model. These findings suggest that Marein may
467 have considerable potential for preventing high glucose-induced glucose
468 metabolism disorder and IR.

469 **Acknowledgements**

470 The work was supported by grants from the National Natural Science
471 Foundation of China (8010907, 81271255 and 81274188), 973 Program
472 (2013CB531200), the Program for Changjiang Scholars and Innovative
473 Research Team (IRT1150). China HiTech 863 Program (2012AA020205,

2014AA020906), Instrumentation Program of Ministry of Science and Technology of China (2012YQ18011710), Young Scientist Grant from Peking Union Medical College (2012J22), CAMS Innovation Fund for Medical Sciences (CIFMS 2016-I2M-1-012).

Conflict of Interest: We wish to confirm that there are no known conflicts of interest associated with this publication and there has been no significant financial support for this work that could have influenced its outcome.

Author Contributions:

Conceptualization: G,Xiao.

Data curation: B,Jiang.

Formal analysis: LLe.

Investigation: B,Jiang.

Methodology: LLe.

Project administration: L, Xu K,Hu

Resources: L, Xu.

Software: B,Jiang.

Supervision: G,Xiao.

Validation: G,Xiao.

Visualization: L, Xu K,Hu.

Writing – original draft: LLe B,Jiang.

Writing – review & editing: LLe B,Jiang.

References:

1. Pozzilli P, Leslie RD, Chan J, et al. The A1C and ABCD of glycaemia management in type 2 diabetes: a physician's personalized approach. Diabetes Metab Res Rev, 2010, **26 (4)**: 239-

244.
2. Matsuoka T, Kajimoto Y, Watada H, et al. Glycation-dependent, reactive oxygen species-mediated suppression of the insulin gene promoter activity in HIT cells. J Clin Invest, 1997, **99 (1)**: 144-150.
3. Abdul-Ghani MA, Williams K, DeFronzo RA, et al. What is the best predictor of future type 2 diabetes? Diabetes Care, 2007, **30 (6)**: 1544-1548.
4. Rossetti L. Glucose toxicity: the implications of hyperglycemia in the pathophysiology of diabetes mellitus. Clin Invest Med, 1995, **18 (4)**: 255-260.
5. Copeland RJ, Bullen JW, and Hart GW. Cross-talk between GlcNAcylation and phosphorylation: roles in insulin resistance and glucose toxicity. Am J Physiol Endocrinol Metab, 2008, **295 (1)**: E17-28.
6. Konig M, Bulik S, and Holzhutter HG. Quantifying the contribution of the liver to glucose homeostasis: a detailed kinetic model of human hepatic glucose metabolism. PLoS Comput Biol, 2012, **8 (6)**: e1002577.
7. Frantz ED, Penna-de-Carvalho A, Batista Tde M, et al., *Comparative effects of the renin-angiotensin system blockers on nonalcoholic fatty liver disease and insulin resistance in C57BL/6 mice*, in *Metab Syndr Relat Disord*. 2014. p. 191-201.
8. Wang J, Liu B, Han H, et al. Acute hepatic insulin resistance contributes to hyperglycemia in rats following myocardial infarction. Mol Med, 2015.
9. Ferrannini E, Natali A, Camastra S, et al. Early metabolic markers of the development of dysglycemia and type 2 diabetes and their physiological significance. Diabetes, 2013, **62 (5)**: 1730-1737.
10. Zhou J, Xu G, Yan J, et al. Rehmannia glutinosa (Gaertn.) DC. polysaccharide ameliorates hyperglycemia, hyperlipemia and vascular inflammation in streptozotocin-induced diabetic mice. J Ethnopharmacol, 2015, **164**: 229-238.
11. Wang C, Chen Z, Li S, et al. Hepatic overexpression of ATP synthase beta subunit activates PI3K/Akt pathway to ameliorate hyperglycemia of diabetic mice. Diabetes, 2014, **63 (3)**: 947-959.
12. Lee YS, Lee EK, Oh HH, et al. Sodium meta-arsenite ameliorates hyperglycemia in obese diabetic db/db mice by inhibition of hepatic gluconeogenesis. J Diabetes Res, 2014, **2014**: 961732.
13. Cnop M, Vidal J, Hull RL, et al. Progressive loss of beta-cell function leads to worsening glucose tolerance in first-degree relatives of subjects with type 2 diabetes. Diabetes Care, 2007, **30 (3)**: 677-682.
14. Mendez-Lucas A, Hyrossova P, Novellasdemunt L, et al. Mitochondrial phosphoenolpyruvate carboxykinase (PEPCK-M) is a pro-survival, endoplasmic reticulum (ER) stress response gene involved in tumor cell adaptation to nutrient availability. J Biol Chem, 2014, **289 (32)**: 22090-22102.
15. Nicholson JK, Connelly J, Lindon JC, et al. Metabonomics: a platform for studying drug toxicity and gene function. Nat Rev Drug Discov, 2002, **1 (2)**: 153-161.
16. Suhre K. Metabolic profiling in diabetes. J Endocrinol, 2014, **221 (3)**: R75-85.
17. Kim K, Aronov P, Zakharkin SO, et al. Urine metabolomics analysis for kidney cancer detection and biomarker discovery. Mol Cell Proteomics, 2009, **8 (3)**: 558-570.
18. Cheng S, Rhee EP, Larson MG, et al. Metabolite profiling identifies pathways associated with metabolic risk in humans. Circulation, 2012, **125 (18)**: 2222-2231.
19. Floegel A, Stefan N, Yu Z, et al. Identification of serum metabolites associated with risk of type 2 diabetes using a targeted metabolomic approach. Diabetes, 2013, **62 (2)**: 639-648.
20. Dias T, Liu B, Jones P, et al. Cytoprotective effect of Coreopsis tinctoria extracts and flavonoids on tBHP and cytokine-induced cell injury in pancreatic MIN6 cells. J Ethnopharmacol, 2012, **139 (2)**: 485-492.
21. Srere PA. Isotope studies on citrate-condensing enzyme. Adv Tracer Methodol, 1966, **3**: 199-209.
22. Jiang B, Le L, Wan W, et al. The Flower Tea Coreopsis tinctoria Increases Insulin Sensitivity and Regulates Hepatic Metabolism in Rats Fed a High-Fat Diet. Endocrinology, 2015, **156 (6)**: 2006-2018.
23. Zhang Y SS, Zhao M, Jiang Y, Tu P. . A novel chalcone from *Coreopsis tinctoria* Nutt. Biochem Syst Ecol 2006, **34: (766–769.)**.

24. Liang SH, Pang SB, Liu XY, et al. Laboratory study of Coreopsis extracts on reducing blood lipid in hyperlipimia model mice. Journal of Nongken Medicine 2009, **31**: 495-498.
25. Lan S, Lin J, and Zheng N. Evaluation of the antioxidant activity of coreopsis tinctoria nuff. And optimisation of isolation by response surface methodology. Acta Pharm, 2014, **64 (3)**: 369-378.
26. Dias T, Mota-Filipe H, Liu B, et al. Recovery of oral glucose tolerance by Wistar rats after treatment with Coreopsis tinctoria infusion. Phytother Res, 2010, **24 (5)**: 699-705.
27. Ming T, Sun HY, Hu MY, et al. Experimental study on antihypertension and in vivo antioxidant function of Coreopsis extract. Chinese Journal of Experimental Traditional Medical Formulae 2012, **18**: 249-252.
28. Dias T, Bronze MR, Houghton PJ, et al. The flavonoid-rich fraction of Coreopsis tinctoria promotes glucose tolerance regain through pancreatic function recovery in streptozotocin-induced glucose-intolerant rats. J Ethnopharmacol, 2010, **132 (2)**: 483-490.
29. Jiang BP, Le L, Yao X, et al. Establishment of Insulin Resistance HepG2 Cell Model and Its Application in Screening Bioactive Components of *Coreopsis tinctoria*. Mod Chin Med, 2017, **19**: 165-173.
30. Jiang B, Le L, Zhai W, et al. Protective effects of marein on high glucose-induced glucose metabolic disorder in HepG2 cells. Phytomedicine, 2016, **23 (9)**: 891-900.
31. Srere PA and Foster DW. On the proposed relation of citrate enzymes to fatty acid synthesis and ketosis in starvation. Biochem Biophys Res Commun, 1967, **26 (5)**: 556-561.
32. Iizuka K, Bruick RK, Liang G, et al. Deficiency of carbohydrate response element-binding protein (ChREBP) reduces lipogenesis as well as glycolysis. Proc Natl Acad Sci U S A, 2004, **101 (19)**: 7281-7286.
33. Yoshioka K, Saito M, Oh KB, et al. Intracellular fate of 2-NBDG, a fluorescent probe for glucose uptake activity, in Escherichia coli cells. Biosci Biotechnol Biochem, 1996, **60 (11)**: 1899-1901.
34. MacDonald MJ, Brown LJ, Longacre MJ, et al. Knockdown of both mitochondrial isocitrate dehydrogenase enzymes in pancreatic beta cells inhibits insulin secretion. Biochim Biophys Acta, 2013, **1830 (11)**: 5104-5111.
35. Yuan M, Breitkopf SB, Yang X, et al. A positive/negative ion-switching, targeted mass spectrometry-based metabolomics platform for bodily fluids, cells, and fresh and fixed tissue. Nat Protoc, 2012, **7 (5)**: 872-881.
36. Srere PA. A magnetic resonance study of the citrate synthase reaction. Biochem Biophys Res Commun, 1967, **26 (5)**: 609-614.
37. Klover PJ and Mooney RA. Hepatocytes: critical for glucose homeostasis. Int J Biochem Cell Biol, 2004, **36 (5)**: 753-758.
38. Wang W, Cote J, Xue Y, et al. Purification and biochemical heterogeneity of the mammalian SWI-SNF complex. EMBO J, 1996, **15 (19)**: 5370-5382.
39. Cline GW, Petersen KF, Krssak M, et al. Impaired glucose transport as a cause of decreased insulin-stimulated muscle glycogen synthesis in type 2 diabetes. N Engl J Med, 1999, **341 (4)**: 240-246.
40. Iyer VV, Yang H, Ierapetritou MG, et al. Effects of glucose and insulin on HepG2-C3A cell metabolism. Biotechnol Bioeng, 2010, **107 (2)**: 347-356.
41. Nibourg GA, Huisman MT, van der Hoeven TV, et al. Stable overexpression of pregnane X receptor in HepG2 cells increases its potential for bioartificial liver application. Liver Transpl, 2010, **16 (9)**: 1075-1085.
42. Tian N, Wang JS, Wang PR, et al. NMR-based metabonomic study of Chinese medicine Gegen Qinlian Decoction as an effective treatment for type 2 diabetes in rats. Metabolomics, 2013, **9 (6)**: 1228-1242.
43. Byun JK, Choi YK, Kang YN, et al. Retinoic acid-related orphan receptor alpha reprograms glucose metabolism in glutamine-deficient hepatoma cells. Hepatology, 2015, **63 (3)**: 953-964.
44. Ortenblad N, Mogensen M, Petersen I, et al. Reduced insulin-mediated citrate synthase activity in cultured skeletal muscle cells from patients with type 2 diabetes: evidence for an intrinsic oxidative enzyme defect. Biochim Biophys Acta, 2005, **1741 (1-2)**: 206-214.
45. Ishii N, Carmines PK, Yokoba M, et al. Angiotensin-converting enzyme inhibition curbs tyrosine nitration of mitochondrial proteins in the renal cortex during the early stage of diabetes mellitus in rats. Clin Sci (Lond), 2013, **124 (8)**: 543-552.

46. Choi SE, Lee YJ, Hwang GS, et al. Supplement of TCA cycle intermediates protects against high glucose/palmitate-induced INS-1 beta cell death. Arch Biochem Biophys, 2011, **505 (2)**: 231-241.

Figures and Legends

Figure 1 AC improves serum glucose and lipid homeostasis and protects against HFD-induced IR. The serum levels of TC (A), TG (B), LDL-C (C), HDL-C (D), fasting blood glucose (E), fasting insulin (F) were measured. G, Insulin sensitivity index [ISI =1/(fasting insulin × fasting plasma glucose)]. H, insulin tolerance tests (ITT). I, body weight Values are the means ± SEM (n = 10). .* *P<0.05* vs the control group; ** *P<0.01* vs the control group; # *P<0.05* vs HFD-treated group; ## *P<0.01* vs HFD-treated group.

Figure 2 Effects of AC on lipid accumulation and steatosis. Representative hematoxylin and eosin staining of the liver (magnifications, ×200).

Figure 3 Marein inhibits the decrease of glucose uptake and the imbalance of glucose metabolism induced by high glucose in HepG2 cells. (A) Dose-dependent and time-dependent effect of glucose on 2-NBDG uptake. (B) Dose-dependent effect of Marein on 2-NBDG uptake. HepG2 cells were incubated for 24h. (C) Glucose uptake expressed as a percent of control group are means ± SD of at least 4 different samples per condition. (D) Cell viability shows the toxicological effect of Marein in HepG2 cells. (E) Effect of Marein on glycogen content. (F) Effect of Marein on Hexokinase activity. (G)

642 Bands of representative experiments for PEPCK and G6Pase. (H)
643 Densitometric quantification of PEPCK and G6Pase. (I) Effect of Marein on
644 mRNA expression of PEPCK and G6Pase. All experiments were performed at
645 least 4 times. * *P<0.05* vs the control group; ** *P<0.01* vs the control group;***
646 *P<0.001* vs the control group; # *P<0.05*vs 55 mmol/L glucose-treated group;
647 ## *P<0.01* vs 55 mmol/L glucose-treated group.
648
649 **Figure 4** PCA scores plots for HPLC/MS data of all groups. (A) The three-
650 dimensional PCA score plot of metabolic states of normal control group (red
651 ●), high glucose group (green ●), 10 μmol/L Marein group (blue ●), 5 μmol/L
652 Marein group (bright blue ●) and Positive control group (pink ●). (B) The
653 three-dimensional PCA score plot of metabolic states of normal control group
654 (red ●) and high glucose group (green ●). (C) The three-dimensional PCA
655 score plot of metabolic states of high glucose group (red ●) and Positive
656 control group (green ●). (D) The three-dimensional PCA score plot of
657 metabolic state of high glucose group (red ●) and 5 μmol/L Marein group
658 (green ●). (E) The three-dimensional PCA score plot of metabolic state of
659 high glucose group (red ●) and 10 μmol/L Marein group (green ●). (F)
660 Summary of pathway analysis with MetPA. Positive control is 0.5 mmol/L
661 metformin.
662
663 **Figure 5** The variance analysis of metabolites based on the data of HPLC/MS
664 of cells. (A) Heat map visualization of the correlation analysis of all
665 metabolites. Row: groups (red: normal control; green: high glucose; blue: 10
666 μmol/L Marein; bright blue: 5 μmol/L Marein; pink: Positive control); columns:

667 metabolites; Cell color key indicates the cluster score, green: Lowest, red:
668 highest. (B) High glucose-based z-score plot of named metabolites for
669 comparison between normal control (black), high glucose (red) and 10 µmol/L
670 Marein (green). Data are shown as standard deviation from the mean of
671 respective sham. Each dot represents a single metabolite in 1 sample; n=4
672 per group.
673
674 **Figure 6** Metabolome pathway map of quantified metabolites, including
675 components of the glycolytic or gluconeogenesis pathway and Krebs cycle in
676 all groups. The red box shows the enzymes increased by high glucose
677 treatment. *$P<0.05$ vs the control group; ** $P<0.01$ vs the control group;***
678 $P<0.001$ vs the control group; # $P<0.05$ vs 55 mmol/L glucose-treated group;
679 ## $P<0.01$ vs 55 mmol/L glucose-treated group. F6P, Fructose 6-phosphate;
680 F1,6P, Fructose 1,6-bisphosphate; DHAP, Dihydroxyacetone phosphate; PEP,
681 Phosphoenolpyruvate;
682
683 **Figure 7** Marein inhibits the increase of mRNA expression and protein levels
684 of Krebs cycle enzymes induced by high glucose in HepG2 cells. (A)Effect of
685 Marein on mRNA expression of Krebs cycle genes. (B) Bands of
686 representative experiments for FH, MDH2, SDHA, SDHB, IDH2, ACO2 and
687 CS. (C) Densitometric quantification of Krebs cycle enzymes. (D) ATP levels
688 expressed as a percent of control group are means ± SD of at least 4 different
689 samples per condition. (E) Effect of Marein on pyruvate concentration. (F)
690 Lactate concentrations expressed as a percent of control group are means ±
691 SD of at least 4 different samples per condition.* $P<0.05$ vs the control group;

692 ** *P<0.01* vs the control group; # *P<0.05* vs 55 mmol/L glucose-treated group;

693 ## *P<0.01* vs 55 mmol/L glucose-treated group.

694

695

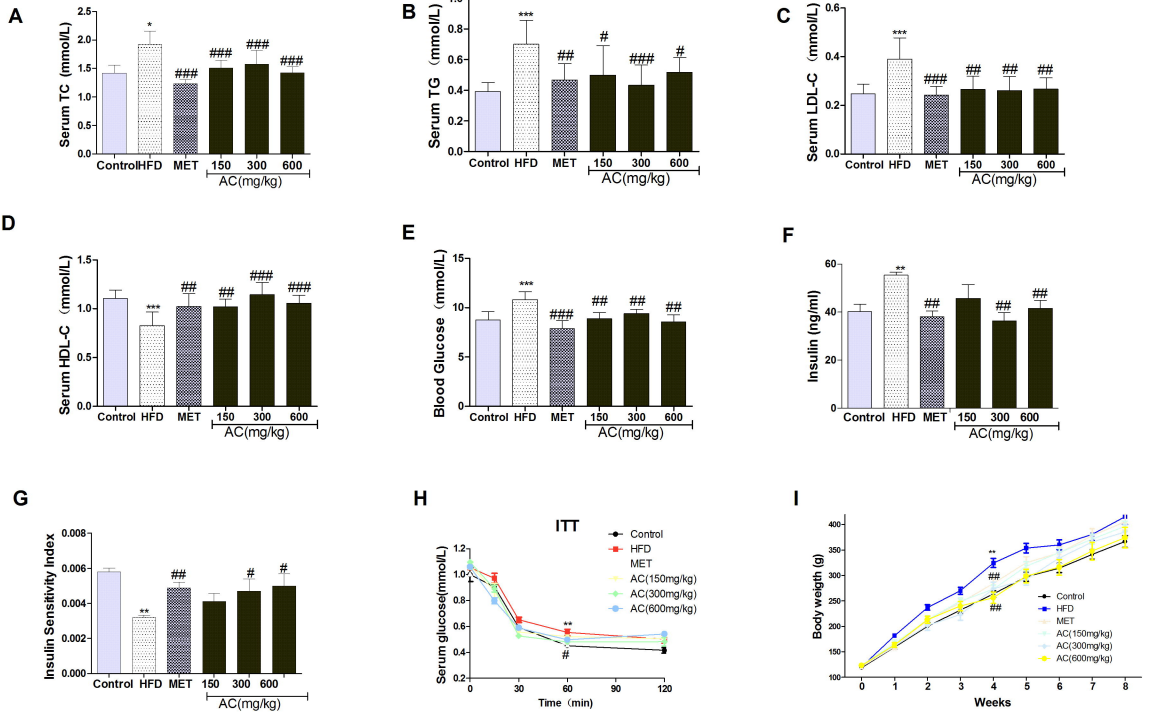
A
Serum TC (mmol/L)
Control HFD MET 150 300 600
AC(mg/kg)
B
Serum TG (mmol/L)
C
Serum LDL-C (mmol/L)
D
Serum HDL-C (mmol/L)
E
Blood Glucose (mmol/L)
F
Insulin (ng/ml)
G
Insulin Sensitivity Index
H
ITT
Control
HFD
MET
AC(150mg/kg)
AC(300mg/kg)
AC(600mg/kg)
Serum glucose(mmol/L)
Time (min)
I
Body weigth (g)
Weeks

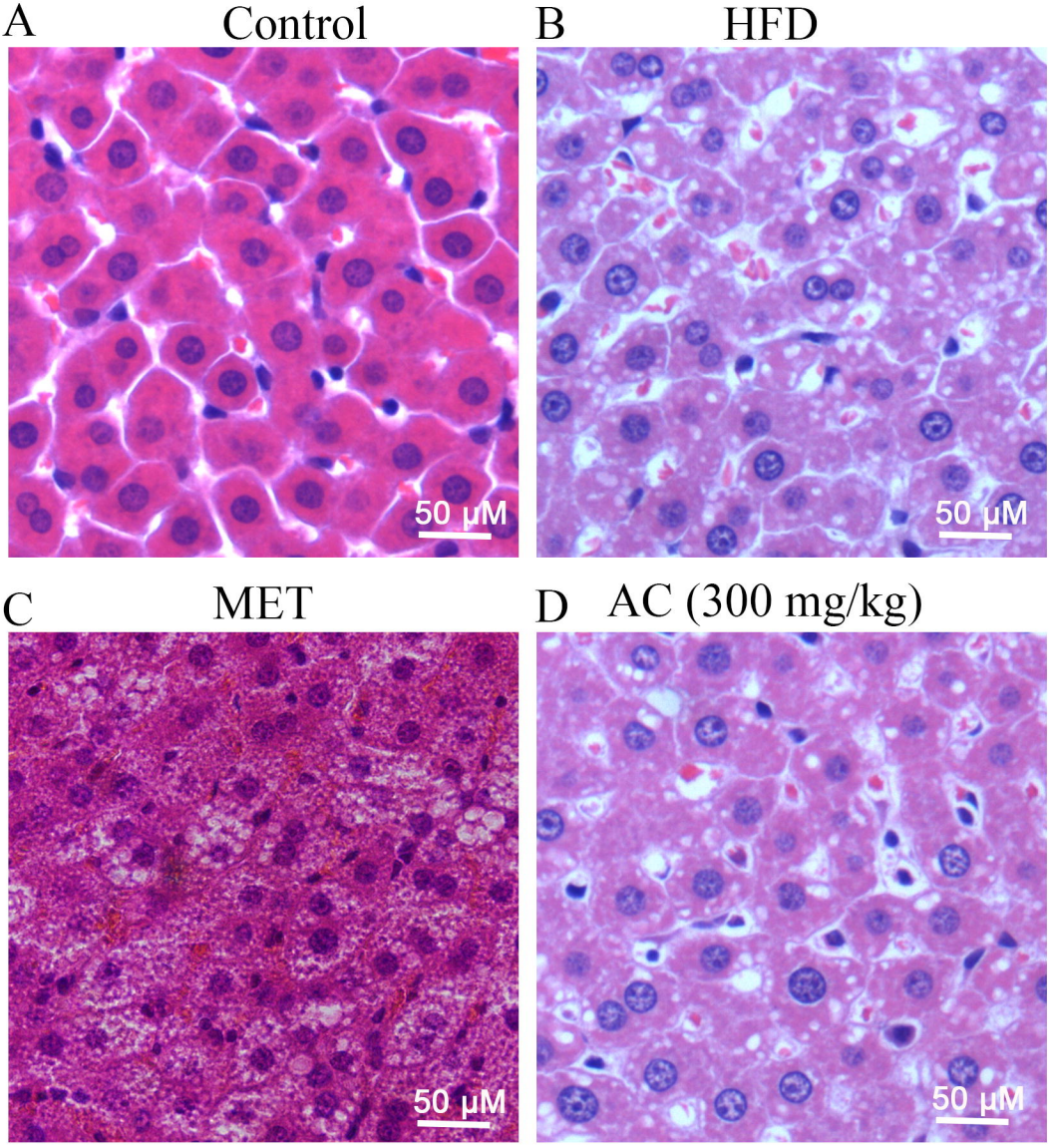
A
Control
50 μM
B
HFD
50 μM
C
MET
50 μM
D
AC (300 mg/kg)
50 μM

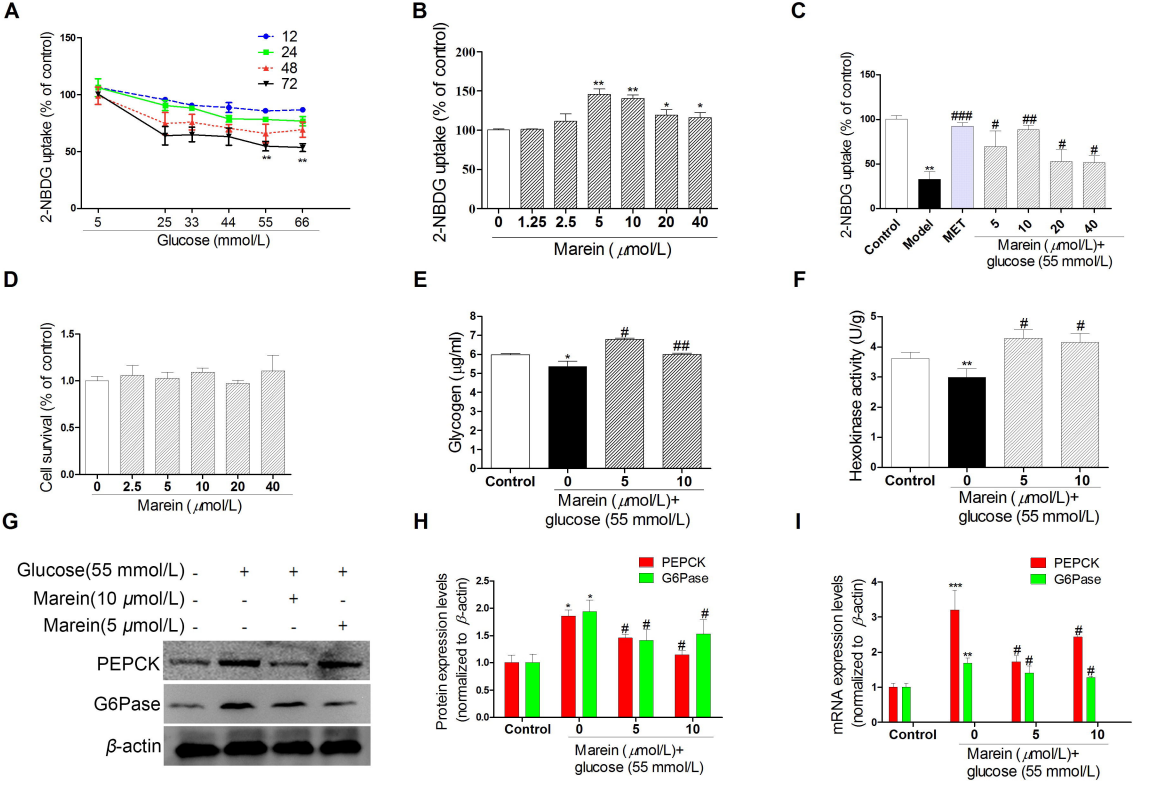
A
2-NBDG uptake (% of control)
12
24
48
72
Glucose (mmol/L)
B
2-NBDG uptake (% of control)
Marein (μmol/L)
C
2-NBDG uptake (% of control)
Control
Model
MET
Marein (μmol/L)+
glucose (55 mmol/L)
D
Cell survival (% of control)
Marein (μmol/L)
E
Glycogen (μg/ml)
Control
Marein (μmol/L)+
glucose (55 mmol/L)
F
Hexokinase activity (U/g)
Control
Marein (μmol/L)+
glucose (55 mmol/L)
G
Glucose(55 mmol/L)
Marein(10 μmol/L)
Marein(5 μmol/L)
PEPCK
G6Pase
β-actin
H
PEPCK
G6Pase
Protein expression levels
(normalized to β-actin)
Control
Marein (μmol/L)+
glucose (55 mmol/L)
I
PEPCK
G6Pase
mRNA expression levels
(normalized to β-actin)
Control
Marein (μmol/L)+
glucose (55 mmol/L)

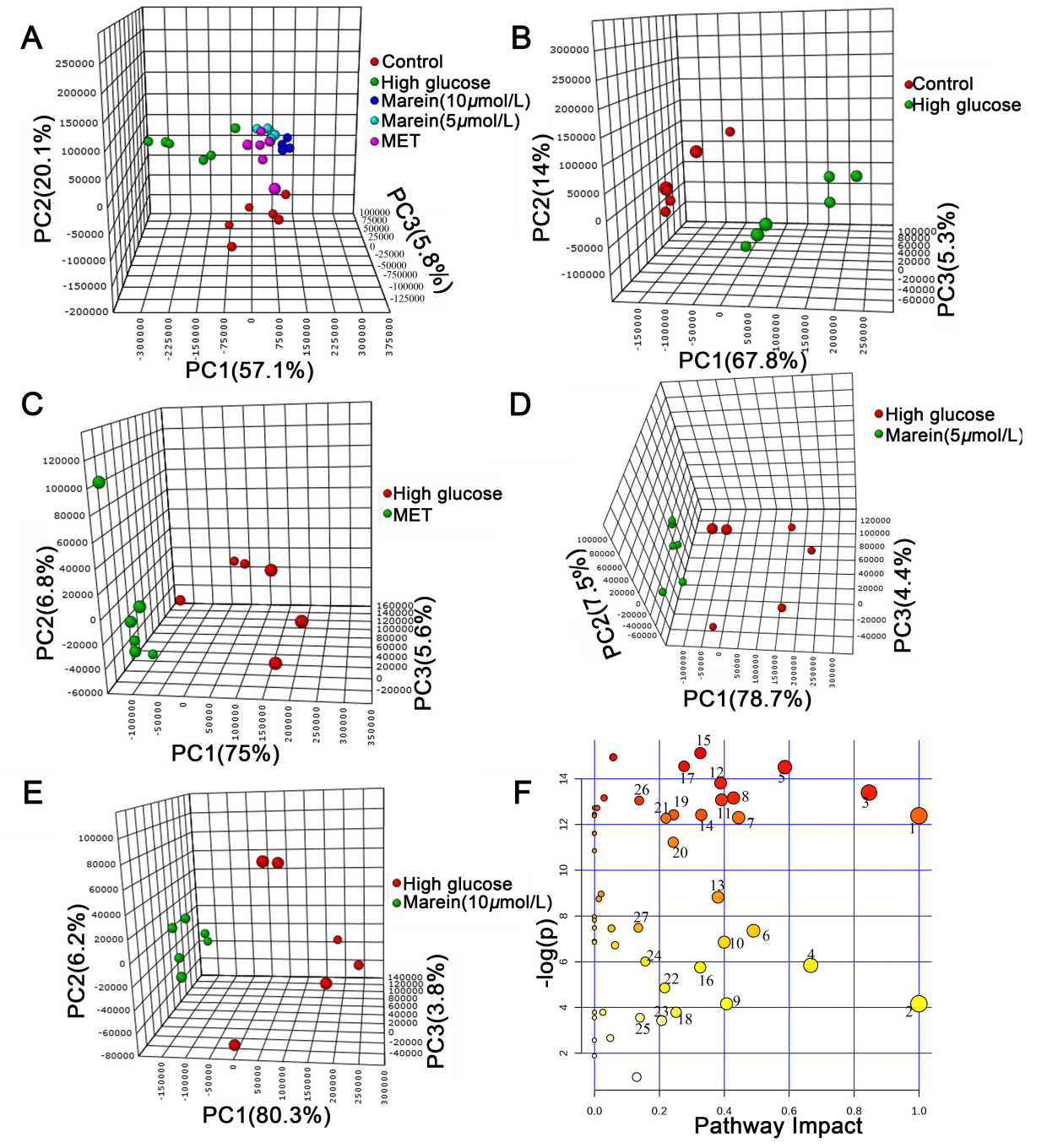
A
Control
High glucose
Marein(10μmol/L)
Marein(5μmol/L)
MET
PC1(57.1%)
PC2(20.1%)
PC3(5.8%)
B
Control
High glucose
PC1(67.8%)
PC2(14%)
PC3(5.3%)
C
High glucose
MET
PC1(75%)
PC2(6.8%)
PC3(5.6%)
D
High glucose
Marein(5μmol/L)
PC1(78.7%)
PC2(7.5%)
PC3(4.4%)
E
High glucose
Marein(10μmol/L)
PC1(80.3%)
PC2(6.2%)
PC3(3.8%)
F
-log(p)
Pathway Impact

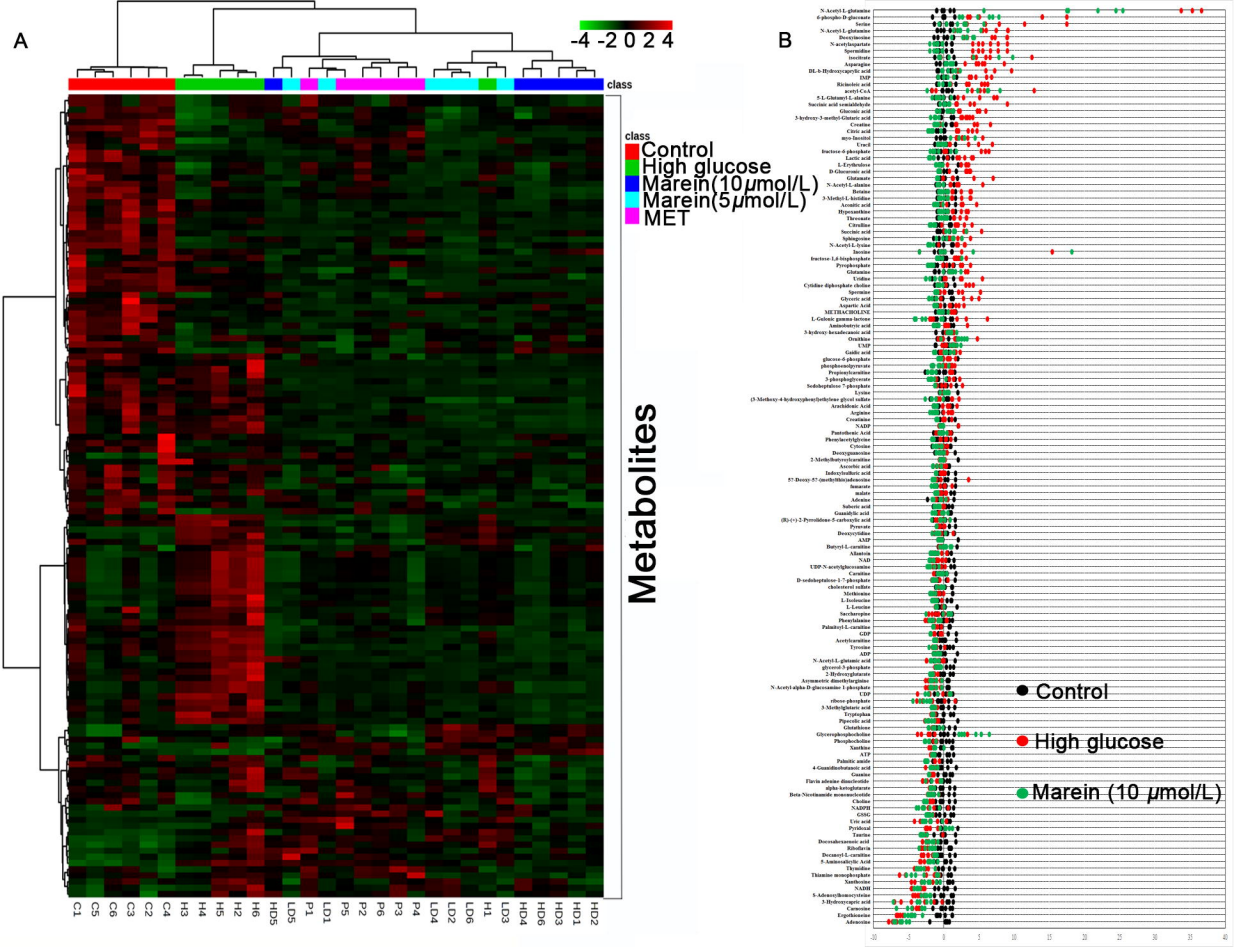
A
-4 -2 0 2 4
class
class
Control
High glucose
Marein(10μmol/L)
Marein(5μmol/L)
MET
Metabolites
C1 C5 C6 C3 C2 C4 H3 H4 H5 H2 H6 HD5 LD5 P1 LD1 P5 P2 P6 P3 P4 LD4 LD2 LD6 H1 LD3 HD4 HD6 HD3 HD1 HD2
B
Control
High glucose
Marein (10 μmol/L)

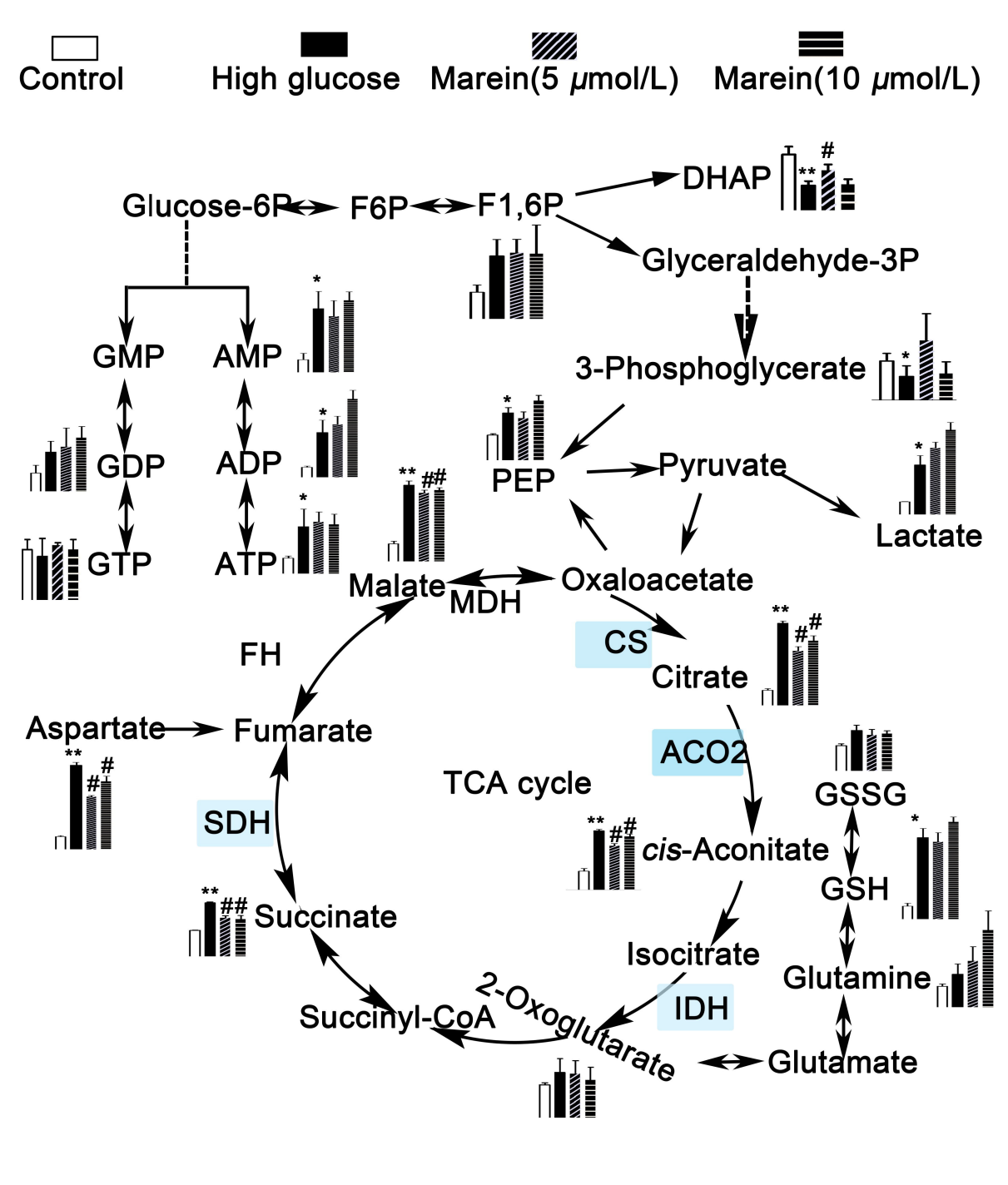
Control
High glucose
Marein(5 μmol/L)
Marein(10 μmol/L)
Glucose-6P
F6P
F1,6P
DHAP
Glyceraldehyde-3P
3-Phosphoglycerate
PEP
Pyruvate
Lactate
GMP
AMP
GDP
ADP
GTP
ATP
Malate
MDH
Oxaloacetate
CS
Citrate
FH
Aspartate
Fumarate
ACO2
TCA cycle
SDH
cis-Aconitate
GSSG
GSH
Succinate
Isocitrate
Glutamine
2-Oxoglutarate
IDH
Succinyl-CoA
Glutamate

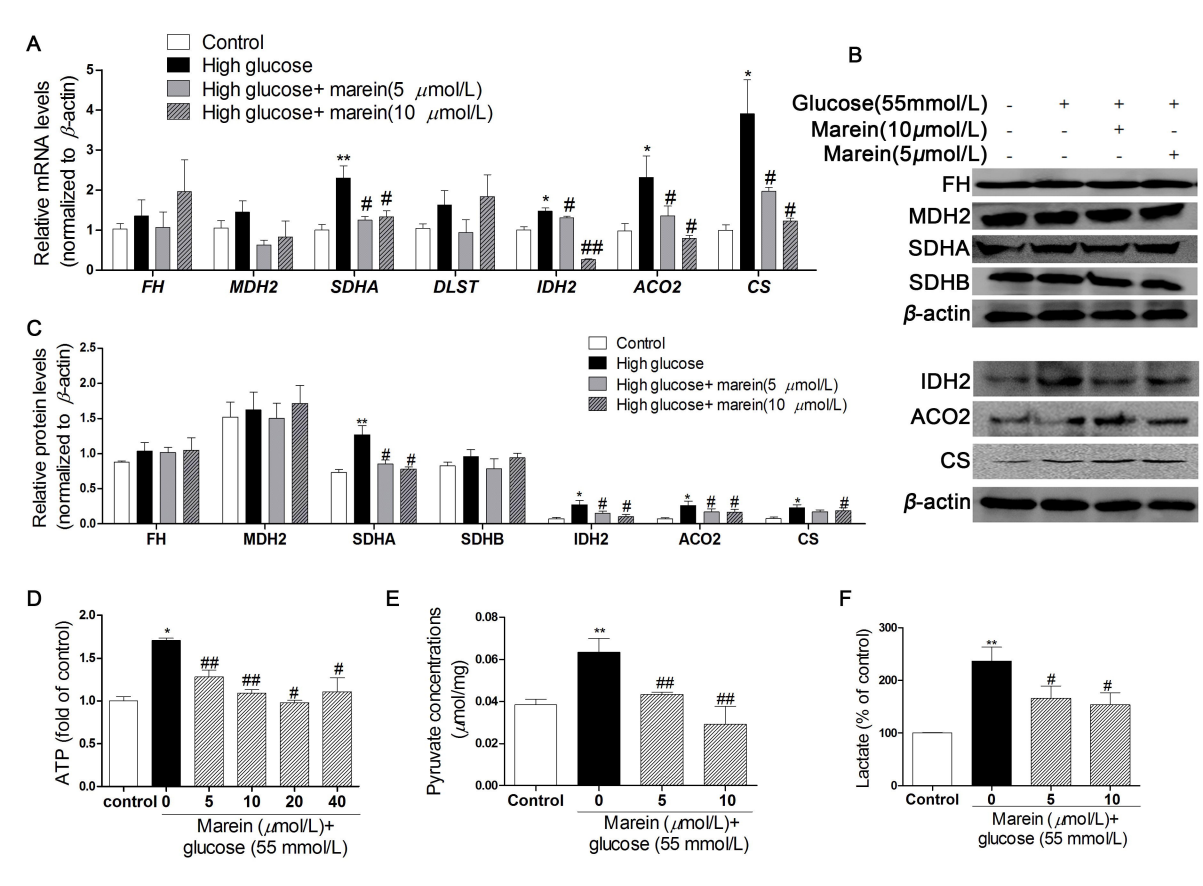
A
Control
High glucose
High glucose+ marein(5 μmol/L)
High glucose+ marein(10 μmol/L)
Relative mRNA levels (normalized to β-actin)
FH
MDH2
SDHA
DLST
IDH2
ACO2
CS
B
Glucose(55mmol/L)
Marein(10μmol/L)
Marein(5μmol/L)
FH
MDH2
SDHA
SDHB
β-actin
IDH2
ACO2
CS
β-actin
C
Control
High glucose
High glucose+ marein(5 μmol/L)
High glucose+ marein(10 μmol/L)
Relative protein levels (normalized to β-actin)
FH
MDH2
SDHA
SDHB
IDH2
ACO2
CS
D
ATP (fold of control)
control
0
5
10
20
40
Marein (μmol/L)+ glucose (55 mmol/L)
E
Pyruvate concentrations (μmol/mg)
Control
0
5
10
Marein (μmol/L)+ glucose (55 mmol/L)
F
Lactate (% of control)
Control
0
5
10
Marein (μmol/L)+ glucose (55 mmol/L)